Adlayer Structures of Chlorine, Bromine, and Iodine on Cu(111) Electrode in Solution: In-Situ STM and ex-Situ LEED Studies

J. Inukai, Y. Osawa, and K. Itaya*

Department of Applied Chemistry, Graduate School of Engineering, Tohoku University, Aoba-yama 04, Sendai 980-8579, Japan

Received: July 10, 1998; In Final Form: October 8, 1998

Adlayer structures of Cl, Br, and I on the Cu(111) surface have been investigated using in-situ scanning tunneling microscopy (STM) in solution and ex-situ low-energy electron diffraction (LEED) in ultrahigh vacuum. The atomic structure of Cu(111)−(1 × 1) was observed by in-situ STM in a perchloric acid solution. Complementary use of LEED and in-situ STM revealed ($p \times \sqrt{3}$) centered-rectangular phases for Cl and Br, in which the structures are compressed almost linearly with potential. In the case of iodine monolayer, a ($\sqrt{3} \times \sqrt{3}$)*R*30° structure was consistently observed in the potential range investigated. The compression in the adlayers of Cl and Br on Cu(111) can be explained in terms of the difference in their van der Waals diameters.

Introduction

It is well-known that chloride, bromide, and iodide ions are strongly adsorbed on various electrode surfaces and play important roles in electrochemical reactions. The structures of halogen adlayers, particularly iodine on well-defined Pt, Pd, Rh, Au, and Ag, have been investigated by tandem ultrahigh-vacuum electrochemical instrumentation (UHV-EC).[1−6] Several commensurate structures of the iodine adlayer on Pt(111),[1,2] Pd(111),[5] and Rh(111)[6] reported previously based on low-energy electron diffraction (LEED) have more recently been investigated further by in-situ scanning tunneling microscopy (STM) in solution.[7−13] In general, the results obtained by in-situ STM for the above system are consistent with those found by LEED. In-situ STM revealed the (3 × 3) and ($\sqrt{7} \times \sqrt{7}$)*R*19.1° structures for Pt(111)[7,12] and the ($\sqrt{3} \times \sqrt{3}$)*R*30° structure for Pd(111)[13] and Rh(111).[11]

On the other hand, it has recently been recognized that the structures of iodine adlayers on Au(111) and Ag(111) are more complicated than those on Pt(111), Pd(111), and Rh(111). At the Au(111) surface, two distinct incommensurate phases were identified and characterized using surface X-ray scattering (SXS) measurements.[14] We have also investigated this system by complementary use of LEED and in-situ STM and obtained results almost identical to those of SXS.[15−17] The adlattices of iodine on Au(111) exhibited two phases, c($p \times \sqrt{3}R-30°$) and rotated-hexagonal ($\sqrt{3}r \times \sqrt{3}r$)*R*(30° + α°), which appeared in negative and positive potential ranges, respectively.[15] In both phases the lattices of the adlayers were compressed when the electrode potential was scanned in the positive direction, the so-called electrocompression.[14] The same behavior was found for the iodine adlayers on Ag(111) in HI[18] and NaI[19] solutions, although more complicated phases were observed in an alkaline solution.[18]

We anticipate that the appearance of the compressed and incommensurate structures of iodine is expected to occur at the fcc (111) surfaces not only for Au(111) and Ag(111) as described above but also for other metal surfaces such as Cu(111). Indeed, it has recently been demonstrated in our study of the underpotential deposition (UPD) of Cu on iodine-modified Pt(111) that the iodine adlayer on the (1 × 1) monolayer of Cu on Pt(111) formed after completion of the UPD reaction also exhibits an incommensurate c($p \times \sqrt{3}R-30°$) structure.[12]

In this respect, the Cu(111) surface is of interest in investigating adlayer structures of halides at the electrode−electrolyte interface. It should be noted that highly ordered adlayers of aromatic molecules such as benzene, naphthalene, and anthracene are formed on Cu(111), while disordered adlayers of these molecules are produced on Pt(111).[20] The adsorption of halides, particularly Cl, has intensively been investigated in UHV using LEED,[21−23] X-ray absorption spectroscopy,[24] and STM.[25]

Goddard and Lambert first performed a systematic study of adlayer structures of Cl on Cu(111) using LEED, reporting several structures including ($\sqrt{3} \times \sqrt{3}$)*R*30°, ($6\sqrt{3} \times 6\sqrt{3}$)*R*30°, and ($12\sqrt{3} \times 12\sqrt{3}$)*R*30°.[21] The LEED pattern for the ($6\sqrt{3} \times 6\sqrt{3}$)*R*30° structure showed a splitting into three spots, triads, and shifted from the ($\sqrt{3} \times \sqrt{3}$)*R*30° spots. Although they concluded from the LEED pattern that the ($6\sqrt{3} \times 6\sqrt{3}$)*R*30° structure was one of the stable adlayers of iodine on Cu(111), we noted that the LEED pattern reported by Goddard and Lambert is very similar to that found for the iodine adsorbed on Au(111), as shown in our previous paper, in which we concluded that the structure should be designated as c($p \times \sqrt{3}R-30°$), the so-called c($p \times \sqrt{3}$).[15,17]

In this paper, we propose new structural models based on in-situ STM and LEED results, in which the Cl and Br adlayers possess the c($p \times \sqrt{3}R-30°$) structure and that of I results in the ($\sqrt{3} \times \sqrt{3}$)*R*30° structure, regardless of the electrode potential.

Experimental Section

Preparation of Clean Cu(111). A commercial Cu(111) single-crystal disk with a diameter of 5 mm (MaTecK-Material-Technolgie & Kristalle GmbH, Germany) was used as the substrate for electrochemical, in-situ STM, and ex-situ LEED measurements. The crystal was metallographically polished and sequentially sonicated in acetone, methanol, and pure water.

10.1021/jp982952l CCC: $15.00
Published on Web 11/12/1998

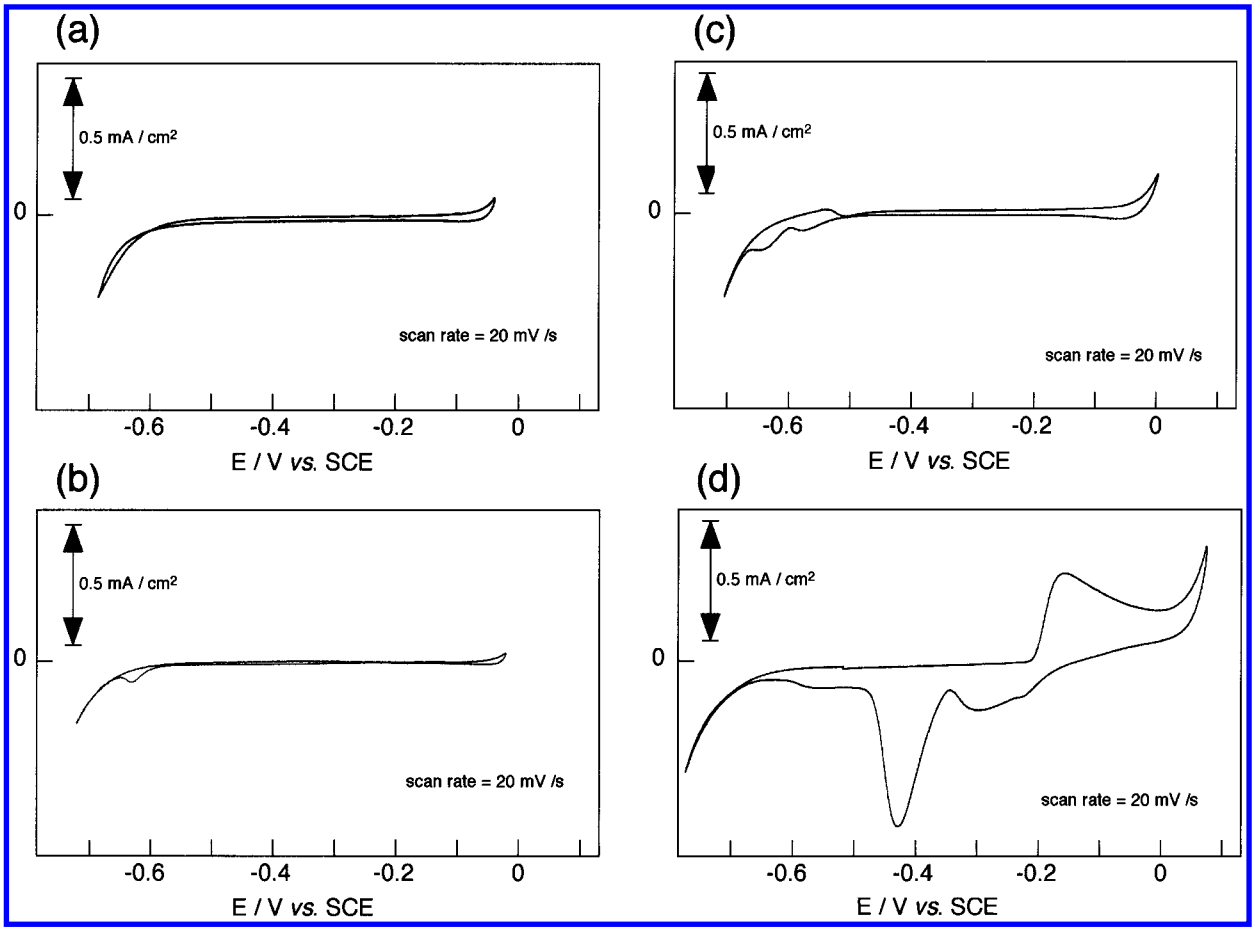

Figure 1. Cyclic voltammograms for Cu(111) electrode in 0.1 M $HClO_4$ (a), 0.1 M $HClO_4$ + 1 mM HCl (b), 0.1 M $HClO_4$ + 1 mM KBr (c), and 0.1 M $HClO_4$ + 1 mM KI (d). Scan rate = 20 mV s^{-1}.

To remove the contaminated surface oxide layers, the Cu(111) surface was electropolished in a mixed solution of phosphoric and sulfuric acids (60 mL of 85% H_3PO_4, 10 mL of concentrated H_2SO_4, and 40 mL of pure water) at ca. 5 A cm^{-2} for 0.1 s. This process produced a mirrorlike surface. The crystal was then rinsed repeatedly with ultrapure Millipore water, and a droplet of water was left on the electrode surface to protect it from contamination during transfer to an electrochemical cell, an in-situ STM cell, or an electrochemical cell attached to the ultrahigh-vacuum chamber. A well-defined single-crystal surface was prepared by anodic dissolution. It has been reported that the anodic dissolution of Cu(111) in pure $HClO_4$ proceeds in the layer-by-layer mode, exposing atomically flat terraces over a large area.[20] For this final etching to produce atomically flat surfaces, we used a 0.1 M $HClO_4$ solution. For the investigation of the structures of halides, the $HClO_4$ solution was replaced by a solution containing HCl, KBr, or KI in each cell with the potential maintained more negative than the open-circuit potential (OCP).

In-Situ Measurements. Electrochemical measurements were carried out in a three-compartment glass cell using 0.1 M $HClO_4$ containing 1 mM of a halide (Cl^-, Br^-, or I^-). Solutions were deoxygenated by bubbling purified N_2.

In-situ STM measurements were carried out with a Nanoscope E (Digital Instruments) using 0.01 M $HClO_4$ containing 0.1 mM of a halide. The STM tips used were made of electrochemically etched tungsten wires. To minimize residual background currents, the side wall of the tips was coated with a nail polish.[17]

Ex-Situ LEED. LEED and Auger electron spectroscopy (AES) experiments were performed in a UHV system consisting of analysis, preparation, and electrochemical (EC) chambers as described previously.[12,15−18] The analysis chamber was equipped with a retarding-field optics for LEED and AES (Omicron Vakuumphysik GmbH, Germany). The Cu(111) substrate was immersed in 0.01 M $HClO_4$ containing 0.1 mM of a halide in the EC chamber backfilled with ultrapure Ar prepared by using a high-temperature Ti-getter chamber. The Cu(111) electrode was set at a certain potential for 30 min, emersed from the electrolyte solution, and then transferred into the analysis chamber. After LEED measurements, AES was carried out to ascertain that there was not a significant amount of impurities such as carbon.

Solutions were prepared with $HClO_4$ (Cica-MERCK, Ultrapur grade), HCl, KBr, KI (KANTO CHEMICAL, Cica-Reagent grade), and ultrapure water (Millipore-Q). The reference electrode was a saturated calomel electrode (SCE).

Results and Discussion

Voltammetric Study. We first describe the cyclic voltammetry of Cu(111) in a perchloric acid solution in the absence and presence of Cl^-, Br^-, and I^- and then discuss in-situ STM and ex-situ LEED experiments. Cyclic voltammograms (CVs) of Cu(111) shown in Figure 1 were recorded by using the hanging meniscus method[15] under a nitrogen atmosphere. Figure 1a shows CV for Cu(111) in a pure $HClO_4$ solution. A featureless double-layer region was observed between ca. −0.05 and −0.6 V.[20] The OCP was measured to be ca. −0.05 V. The anodic current starting at ca. −0.05 V (only a few millivolts more anodic than OCP) is due to the anodic dissolution of copper. The cathodic current at ca. −0.65 V is due to the

hydrogen evolution reaction. When 1 mM of HCl was added, a small cathodic peak was observed at ca. −0.6 V before the hydrogen evolution reaction as shown in Figure 1b. This peak was observed only on well-defined Cu(111) electrodes. Such a peak was not reported in the previous study.[26] The cathodic peak seemed to be due to the desorption of chloride from the copper surface which will be discussed later. The anodic current commencing at ca. −0.05 V should be due to the chloride-assisted anodic dissolution of Cu.[26] For bromide, two small cathodic peaks were observed between −0.65 and −0.55 V (Figure 1c). They are ascribed to the desorption of bromine from Cu(111), which will be discussed later based on STM observations. Figure 1d shows the CV for Cu(111) in 0.1 M $HClO_4$ + 1 mM KI. The anodic current commencing at −0.2 V is due to the bulk formation of insoluble CuI. If the anodic scan is limited to −0.2 V, the formation of CuI did not occur, and the reduction current of CuI between −0.2 and −0.5 V did not appear. Under this limited potential scan, a featureless double-layer region was seen between −0.2 and −0.6 V. At potentials more anodic than 0 V, the bulk dissolution of copper is believed to be responsible for the increase in anodic current shown in Figure 1d. The hydrogen evolution reaction is shifted cathodically in the presence of KI, suggesting that the adsorbed iodine might still exist on Cu(111) in the cathodic potential region.

In-Situ STM on Bare Cu(111). To produce an atomically flat Cu(111) surface for STM observation, a freshly polished surface was first immersed in 0.1 M $HClO_4$ at the OCP in the STM electrochemical cell, and the electrode potential was swept negatively at a scan rate of 50 mV s^{-1} to the hydrogen evolution region and then back to the Cu dissolution region.[20] After several such cycles, the electrode was finally held at a potential near the onset of the anodic dissolution. Soon after the above treatment, well-defined terrace-step features were found to develop gradually, as reported previously.[20] Figure 2a shows a large-scale in-situ STM image of the bare Cu(111) electrode in 0.1 M $HClO_4$ at −0.6 V. It is clear that atomically flat terraces are extended over a few hundred nanometers. Steps, mostly monatomic in height, are not usually straight on Cu(111), indicating that there are many kink sites at the step edges. Figure 2b shows a high-resolution STM image acquired on an atomically flat terrace, with a slight 2D-Foulier filtering. The Cu(111) surface has a hexagonal lattice with an angle of 60° between the atomic rows. The observed atomic distance of ca. 0.26 nm corresponds to the lattice constant of Cu(111), 0.256 nm. Clearly, the STM image shown in Figure 2b indicates that the Cu(111) surface has the (1 × 1) structure in $HClO_4$ solution. No reconstructed structure was found in the double-layer potential range. The above results are consistent with our previous observation.[20]

It is noteworthy that LEED experiments were conducted for the Cu(111) electrode emersed from 0.01 M $HClO_4$ at different potentials. However, only dim (1 × 1) spots were observed when the sample was emersed at potentials in the hydrogen evolution region (for example, at ca. −0.8 V). Practically no spots were found at emersion potentials in the double-layer region. AES clearly showed the existence of oxygen on the surface, indicating that the oxidation of the surface took place during the emersion process. Stickney et al. also described a similar difficulty in transferring an oxide-free Cu electrode using UHV-EC.[23]

Structure of Cl Adlayer on Cu(111). The structure of Cl adlayer on Cu(111) has long been investigated in UHV using LEED,[21−23] an X-ray absorption technique,[24] and STM.[25] Suggs and Bard carried out an in-situ STM study of the Cl adlayer on Cu(111) in a HCl solution.[26] They also assumed that the adlayer forms $(6\sqrt{3} \times 6\sqrt{3})R30°$ structure even in solution. However, it must be emphasized that the initially proposed $(6\sqrt{3} \times 6\sqrt{3})R30°$ structure came from the simple fact that each of the $(\sqrt{3} \times \sqrt{3})R30°$ spots was split into three spots in LEED patterns.[21] More recently, Wohlmann et al. examined the Cl adlayer using in-situ STM.[27] They concluded that the Cl adalyer was identified as $(\sqrt{3} \times \sqrt{3})R30°$.[27]

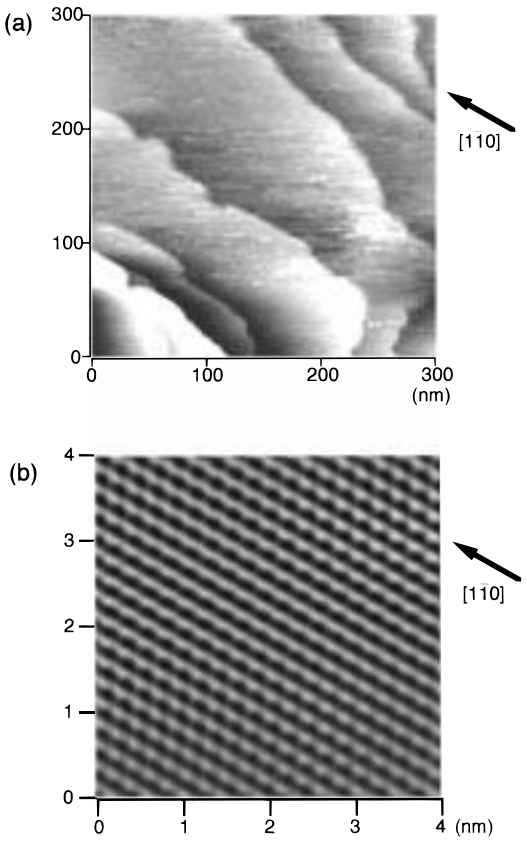

Figure 2. In-situ STM images of Cu(111) surface obtained at −0.6 V in 0.1 M $HClO_4$. Scanned areas: 300 × 300 nm (a) and 4 × 4 nm (b). Tunneling current was 2 nA; tip potenial was −0.3 V.

We made great efforts to determine the adlayer structure as accurately as possible in STM measurements. Atomic images were carefully acquired under minimal drift, which usually caused a distortion in images and a resulting misinterpretation in the determination of unit cells. Figure 3a shows a high-resolution STM image of Cu(111) in 0.01 M $HClO_4$ containing 1 mM HCl acquired at −0.05 V. As reported previously,[26,27] each bright spot is assigned to a Cl atom adsorbed on Cu(111). Note that the Cu(111)-(1 × 1) structure with an almost ideal hexagonal symmetry was obtained, which was similar to the structure shown in Figure 2b, when the potential was scanned more cathodic than the cathodic peak in Figure 1b. After the potential was scanned back to the anodic potential, an identical image for the adsorbed Cl was obtained. Therefore, the small cathodic peak observed at ca. −0.6 V can be assigned to the desorption of adsorbed Cl. The same result was reported by Wohlmann et al.[27]

It can be seen in Figure 3a that there is significant distortion of atomic rows of Cl in the directions labeled L_1, L_2, and L_3. The image cannot be interpreted as the $(\sqrt{3} \times \sqrt{3})R30°$ structure. The atomic distance of Cl atoms along the line L_1 was measured to be 0.44 ± 0.02 nm, $\sqrt{3}$ times the Cu−Cu distance of 0.256 nm. L_1 was rotated by 30 ± 1° with respect

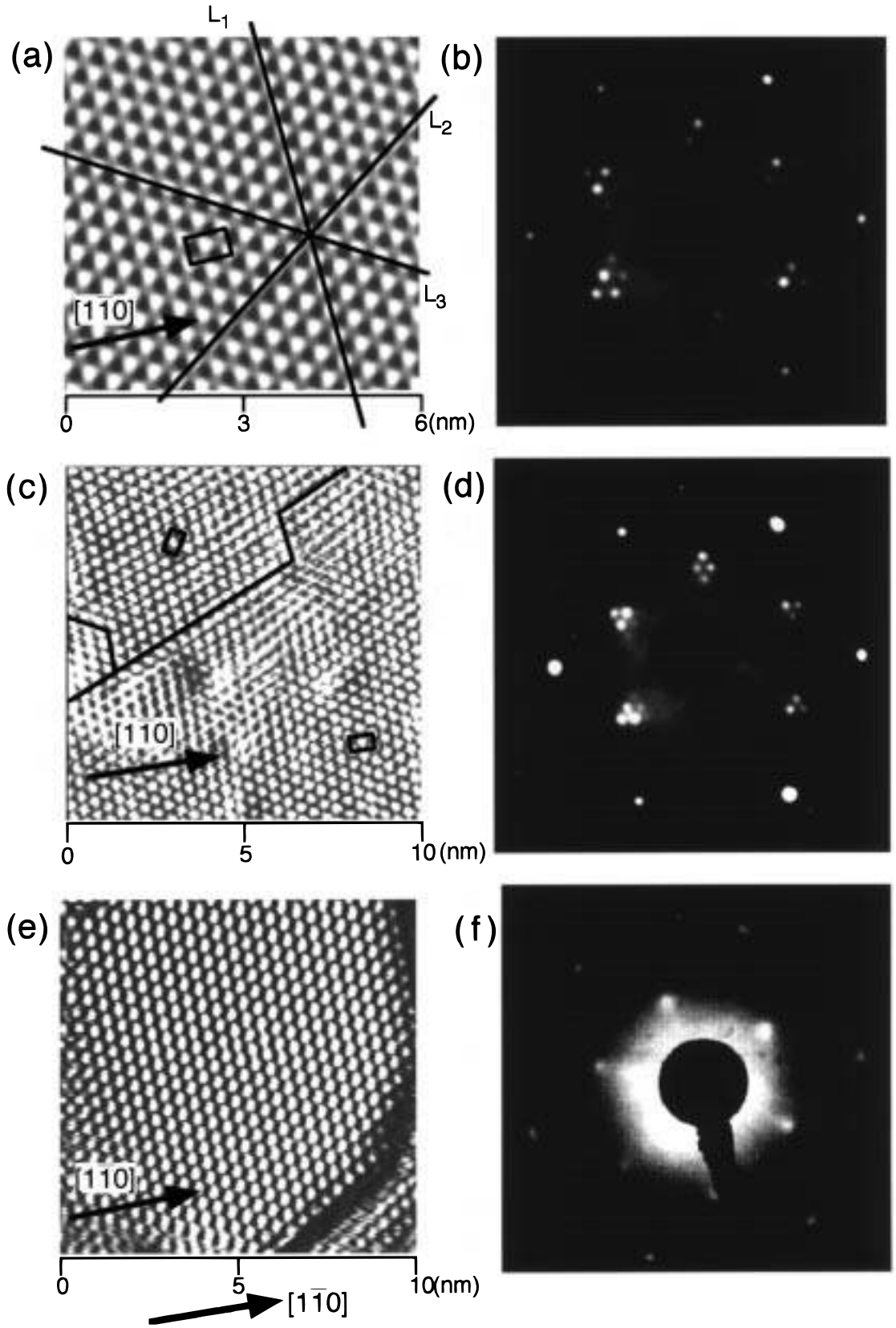

Figure 3. (a) In-situ STM image of Cl adlayer on Cu(111) at −0.05 V in 0.01 M $HClO_4$ + 0.1 mM HCl. Tunneling current was 5 nA. (b) Ex-situ LEED pattern of Cl on Cu(111) emersed from 0.01 M $HClO_4$ + 0.1 mM HCl at −0.05 V. The incident energy was 59.5 eV. (c) In-situ STM image of Br adlayer on Cu(111) at −0.05 V in 0.01 M $HClO_4$ + 0.1 mM KBr. Tunneling current was 5 nA. (d) Ex-situ LEED pattern of Br on Cu(111) emersed from 0.01 M $HClO_4$ + 0.1 mM KBr at −0.05 V. The incident energy was 67.1 eV. (e) In-situ STM image of I adlayer on Cu(111) at −0.5 V in 0.01 M $HClO_4$ + 0.1 mM KI. Tunneling current was 2 nA. (f) Ex-situ LEED pattern of I on Cu(111) emersed from 0.01 M $HClO_4$ + 0.1 mM KI at −0.5 V. The incident energy was 57.4 eV.

to an atomic row of Cu(111). However, the atomic distances between Cl atoms along L_2 and L_3 were almost the same, 0.41 ± 0.02 nm, which is obviously shorter than the atomic distance found along L_1. Moreover, the lines of L_2 and L_3 are rotated

by 57 ± 1° with respect to L_1, and L_2 is rotated by 66 ± 1° with respect to L_3. These angles are different from the angle of 60° predicted for the $(\sqrt{3} \times \sqrt{3})R30°$ structure. These distortions suggest that the lattice unit cell can be defined by the rectangle drawn in Figure 3a. The length of the shorter side is 1.37 ± 0.05 nm, $\sqrt{3}$ times the Cu−Cu distance, while that of the longer side is 2.6 ± 0.1 times the Cu−Cu distance. If the structure in Figure 3a was $(\sqrt{3} \times \sqrt{3})R30°$, the length of the longer side would be exactly 3 times the Cu−Cu distance. It is also important to note that all adsorbed Cl appeared with the same corrugation height. No periodical modulation in the height was observed. This straightforwardly indicates that Cl atoms are located at physically equivalent binding sites. The STM image reported by Suggs and Bard and by Wohlmann et al. also showed a flat feature with no sign of height difference among the Cl adatoms,[26,27] while the image observed in UHV indicated a modulation that was thought to result from the $(6\sqrt{3} \times 6\sqrt{3})R30°$ structure,[25] although detailed analysis of the modulation was not made.

Figure 3b shows a typical LEED pattern of Cu(111) after emersion at −0.05 V. The $(\sqrt{3} \times \sqrt{3})R30°$ spots are now clearly split into three spots, which is consistent with the result reported previously.[21] However, it can also be seen that additional weak spots appear near the three split spots. Besides these detailed features of the LEED pattern, the split spots moved slightly toward the center, and the distances between the split spots decreased when the electrode potential was scanned in the cathodic direction, which will be discussed in a subsequent section. Almost identical LEED patterns were observed for the iodine adlayers on Au(111) and Ag(111) as described previously.[15−18] From the LEED pattern and the in-situ STM images shown in Figure 3a,b, it can be concluded that the adlayer of Cl on Cu(111) possesses the $c(p \times \sqrt{3}R-30°)$ structure rather than the $(6\sqrt{3} \times 6\sqrt{3})R30°$ structure.

A model of the $c(p \times \sqrt{3}R-30°)$ structure is shown in Figure 4a. One side of the rectangular cell is parallel to the $\sqrt{3}$ direction, while the other (p direction) is along the close-packed row of Cu(111). The Cl atoms are compressed only in the direction denoted by p with respect to the $(\sqrt{3} \times \sqrt{3})R30°$ structure. The lengths of the two sides of the adlattice cell are, therefore, $\sqrt{3}$ and p times the Cu−Cu distance, respectively. Since the adlattice is compressed along the p direction, the angle between the two fundamental unit cell vectors of adlattice, $\mathbf{b_1}$ and $\mathbf{b_2}$, is larger than 60° (Figure 4a). Therefore, the angle between the fundamental reciprocal unit cell vectors of adlattice, $\mathbf{b_1}^*$ and $\mathbf{b_2}^*$, is smaller than 120° (Figure 4b). The vector for LEED spots, $\mathbf{r}$, is described as

$$\mathbf{r} = m\mathbf{b_1}^* + n\mathbf{b_2}^* \quad (1)$$

where m and n are integers. When m, $n = -1$, 0, or 1, the LEED spots for the $c(p \times \sqrt{3}R-30°)$ structure are expressed by a compressed hexagon shown by the dashed lines in Figure 4b. As discussed previously,[15] there are three rotational domains for the $c(p \times \sqrt{3}R-30°)$ structure, rotated by 120° from each other. The simulated LEED pattern results from the projection of the reciprocal vectors for the three rotational domains. As the p value becomes smaller, the inner hexagon in Figure 4b becomes more compressed, and the distance between adjacent groups of split spots becomes larger. In this way, the p value was calculated from the LEED pattern shown in Figure 3b. The value obtained is 2.48 ± 0.02, which almost coincides with that obtained by in-situ STM, 2.5 ± 0.1. Walter et al. calculated the heights of the Cl atoms located at atop, bridge, and 3-fold hollow sites on Cu(111).[22] According to their calculations, STM images should be able to distinguish between the atoms located at the different binding sites, whereas the STM shown in Figure 3a indicated that all adatoms appear with the same corrugation height. This suggests that the Cl atoms seem to be located near the traces of "p bisectors" on Cu(111) as discussed previously.[17]

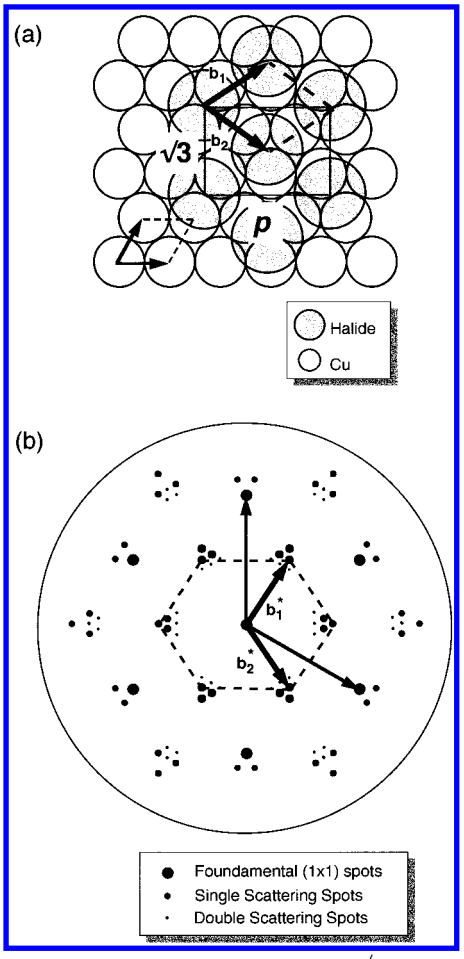

Figure 4. (a) Structural model of the $c(p \times \sqrt{3}R-30°)$ lattice on Cu(111). (b) Calculated LEED pattern for $c(p \times \sqrt{3}R-30°)$ ($p = 2.6$).

Br on Cu(111). Previously reported LEED patterns for the Br adlayer on Cu(111) are similar to those for the Cl adlayer.[28−30] At low coverages, it was reported that the adlattice for Br processes the $(\sqrt{3} \times \sqrt{3})R30°$ structure, which was converted to a $(9\sqrt{3} \times 9\sqrt{3})R30°$ structure at high coverages.[30] Note that the reported LEED pattern for $(9\sqrt{3} \times 9\sqrt{3})R30°$ showed triplets similar to those observed for Cl. From our results for Cl, we expected that the adlayer of Br might have a structure similar to that of Cl, which is the $c(p \times \sqrt{3}R-30°)$ structure.

Figure 3c shows a high-resolution STM image obtained at −0.05 V. It can be seen that there are several domain boundaries indicated by the solid lines. The rectangular unit cell is shown in each domain. The image cannot be interpreted as the $(\sqrt{3} \times \sqrt{3})R30°$ structure, because the longer side of the rectangular unit cell is obviously shorter than 3 times the Cu−Cu distance. It is clearly seen that the two unit cells shown in Figure 3c are rotated from each other by 60°. From the STM image, the p value for the adlayer of Br is measured as 2.6 ± 0.1 at −0.05 V.

The LEED pattern in Figure 3d for the adlayer of Br on Cu(111) shows the characteristic feature of the $c(p \times \sqrt{3}R-30°)$ structure. The $(\sqrt{3} \times \sqrt{3})R30°$ spots are triply split, and the double-scattering spots are clearly observed. The p value is calculated to be 2.6 ± 0.02 from the LEED pattern. These

values obtained by STM and LEED are in good agreement within an experimental error, although the values obtained by LEED are more accurate.

Finally, it is noteworthy that the (1 × 1) structure of Cu(111) was discerned when the electrode potential was set at −0.65 V, indicating that the adsorbed Br was partially or totally desorbed from the surface as expected from the CV shown in Figure 1c.

I on Cu(111). The $(\sqrt{3} \times \sqrt{3})R30°$ structure was exclusively observed for the I adlayer on Cu(111) in UHV, which was confirmed by LEED analysis.[31,32] However, no in-situ STM study has previously been carried out on the adsorption of I on Cu(111).

Figure 3e shows a high-resolution STM image of I on Cu(111). The image was acquired under carefully adjusted conditions in which identical images were consistently observed for at least 15 min with negligible drift. The atom−atom distance of I was 0.44 ± 0.02 nm, which corresponds to $\sqrt{3}$ times the Cu−Cu distance (0.443 nm) on Cu(111). All I atomic rows were rotated by 30 ± 1° with respect to the Cu rows, and they formed almost perfect hexagonal adlattices. These results indicate that the adlayer of I possesses the $(\sqrt{3} \times \sqrt{3})R30°$ structure. When the electrode potential was scanned between −0.25 and −0.65 V, the $(\sqrt{3} \times \sqrt{3})R30°$ structure was consistently observed without any detectable change in STM images. Figure 3f shows a typical LEED pattern obtained at −0.5 V, in which no splitting of the $\sqrt{3}$ spots was observed. Exactly the same LEED pattern was found in the double-layer potential range, indicating that only the $(\sqrt{3} \times \sqrt{3})R30°$ structure is formed on Cu(111) in both solution and UHV. Stickney et al. previously reported the same result.[23]

It is of interest to discuss results of our recent study of the UPD of Cu on an iodine-modified Pt(111). It was shown that a (1 × 1)-Cu adlayer is formed after completion of the UPD on the iodine-modified Pt(111). On the other hand, the I adlayer on top of the Cu monolayer on Pt(111) possesses the $c(p \times \sqrt{3}R-30°)$ structure.[12] The difference between the iodine adlayer structures on Cu(111)-(1 × 1) and (1 × 1) monolayer of Cu on Pt(111) (Cu/Pt(111)) is an interesting aspect to consider. One of the reasons may be the difference in chemical nature between the bulk Cu(111) and the Cu/Pt(111). Although I atoms are directly attached on the Cu atoms on both surfaces, only the first layer consists of Cu atoms in Cu/Pt(111). The chemical nature of the Cu monolayer on Cu/Pt(111) should be different from that of the bulk Cu. On the other hand, geometric differences between the bulk Cu(111) and Cu/Pt(111) must be taken into account. The Cu−Cu distance on Cu(111) is 0.256 nm, while that on Cu/Pt(111) is 0.278 nm, the same as the Pt−Pt distance on Pt(111). In view of the van der Waals diameter of I (0.43 nm), it is reasonable that the $(\sqrt{3} \times \sqrt{3})R30°$ structure is more stable for the I adlayer on Cu(111). Since $\sqrt{3}$ times 0.256 nm (Cu−Cu distance for Cu(111)) is equal to 0.443 nm, the van der Waals diameter is only 3% smaller than the distance between the nearest $\sqrt{3}$ sites on Cu(111). The I monolayer with the $(\sqrt{3} \times \sqrt{3})R30°$ structure is almost the close-packed adlayer on Cu(111). Energetically, I atoms may prefer to stay at the stable $\sqrt{3}$ sites rather than to compress themselves on Cu(111). On the other hand, $\sqrt{3}$ times 0.278 nm (Cu−Cu distance for Cu/Pt(111)) is 12% larger than the van der Waals diameter of I. Therefore, the compression of I can take place because of the open structure on Cu/Pt(111). The observed p value was 2.6 ± 0.05 for the compressed structure of $c(p \times \sqrt{3}R-30°)$ for iodine on Cu/Pt(111),[12] resulting in the nearest I−I distance of 0.43 nm, the same as the van der Waals diameter of iodine. The above results show that the difference in van der Waals diameters of the adsorbed anions plays an important role in determining their adlayer structures.

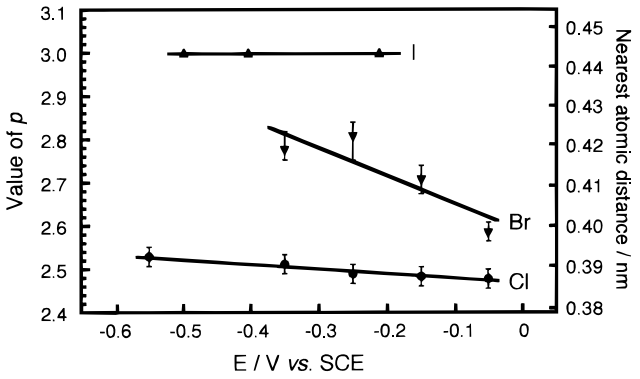

Figure 5. p and the nearest distance in the $c(p \times \sqrt{3}R-30°)$ unit cell as a function of the electrode potential for Cl, Br, and I adlayers.

Potential Dependency. In the case of the adsorbed iodine on Au(111) and Ag(111) electrode surfaces,[14−19] the coverage of iodine increases as the electrode potential is scanned in the positive direction, resulting in the compression of the adlayer. In this study, the potential dependency of lattice parameters in the $c(p \times \sqrt{3}R-30°)$ structure was investigated using LEED for the adlayers of halide ions on Cu(111).

Figure 5 shows the potential dependency of the parameter p and the nearest atomic distance for all adlayers investigated in this study. It is seen that the p value decreases almost linearly with potential for Cl and Br. This behavior is similar to that observed on Au(111) and Ag(111). For Cl, the p value slightly decreases from 2.53 at −0.55 V to 2.48 at −0.05 V. The Cl−Cl distance is calculated as 0.387 nm at −0.05 V, which is close to the van der Waals diameter of Cl, 0.36 nm. For Br, the p value decreases from 2.78 at −0.3 V to 2.59 at −0.05 V. The Br−Br distance at −0.05 V is calculated as 0.399 nm, which is also close to the van der Waals diameter of 0.39 nm. Thus, it is concluded that the compression proceeds when the electrode potential is scanned in the positive direction until the Cl−Cl or Br−Br distances become close to their van der Waals diameters. For I, the p value is independent of the sample potential, $p = 3$, because the adlayer structure is $(\sqrt{3} \times \sqrt{3})R30°$ regardless of the potential, as described above. We recall that the I−I distance at the $\sqrt{3}$ sites is 0.443 nm, and the van der Waals diameter of I is 0.43 nm. Even when the potential is scanned in the positive direction, the compression may be energetically unfavorable to occur. It is clear that the matching of the lattice constant of Cu(111) and the van der Waals diameters of halides is an important factor determining the adlayer structure on electrode surfaces.

One can see in Figure 5 that the potential dependence of compression is greater for Br than Cl. This can also be accounted for in terms of the lattice constant of Cu(111) and the diameter of Br. The van der Waals diameter of Br (0.39 nm) is between Cl (0.36 nm) and I (0.43 nm). Because of this intermediate diameter, Br may possess the characteristics of both I and Cl in regard to the compression. Br is not large enough compared to I to take the $(\sqrt{3} \times \sqrt{3})R30°$ structure at any potential, but it is not as small as Cl to make the compression rate small. More systematic investigations using different substrates are needed to fully understand this phenomenon.

Acknowledgment. This work was supported by a Grant-in-Aid for Research on Priority Area of "Electrochemistry of Ordered Interfaces" (No. 09237101) from the Ministry of

Education, Science, Sports and Culture, Japan, and ERATO-Itaya Electrochemiscopy Project, JST. The authors thank Mr. S. Ibuki for his help in LEED measurements and Dr. Y. Okinaka for his help in the writing of this manuscript.

References and Notes

(1) Hubbard, A. T. *Chem. Rev.* **1988**, *88*, 633.
(2) Lu, F.; Salaita, G. N.; Baltruschat, H.; Hubbard, A. T. *J. Electroanal. Chem.* **1987**, *222*, 305.
(3) Bravo, B. G.; Michelhaugh, S. L.; Soriaga, M. P.; Villegas, I.; Suggs, D. W.; Stickney, J. L. *J. Phys. Chem.* **1991**, *95*, 5245.
(4) Salaita, G. N.; Lu, F.; Laguren-Davison, L.; Hubbard, A. T. *J. Electroanal. Chem.* **1987**, *229*, 1.
(5) Bothwell, M. E.; Cali, G. J.; Berry, G. M.; Soriaga, M. P. *Surf. Sci.* **1991**, *249*, L322.
(6) Hourani, M.; Wasberg, C.; Rhee, C.; Wieckowski, A. *Croat. Chem. Acta* **1990**, *63*, 373.
(7) Schardt, B. C.; Yau, S.-L.; Rinaldi, F. *Science* **1989**, *243*, 1050.
(8) Chang, S.-C.; Yau, S.-L.; Schardi, B. C.; Weaver, M. J. *J. Phys. Chem.* **1991**, *95*, 4787.
(9) Vogel, R.; Kamphausen, I.; Balstuschat, H. *Ber. Bunsen-Ges. Phys. Chem.* **1992**, *96*, 525.
(10) Shinotsuka, N.; Sashikata, K.; Itaya, K. *Surf. Sci.* **1995**, *335*, 75.
(11) Wan, L.-J.; Yau, S.-L.; Swain, G. M.; Itaya, K. *J. Electroanal. Chem.* **1995**, *381*, 105.
(12) Inukai, J.; Osawa, Y.; Wakisaka, M.; Sashikata, K.; Kim, Y.-G.; Itaya, K. *J. Phys. Chem. B* **1998**, *102*, 3498.
(13) Sashikata, K.; Matsui, M.; Itaya, K.; Soriaga, M. P. *J. Phys. Chem.* **1996**, *100*, 20027.
(14) Ocko, B. M.; Watson, G. M.; Wang, J. *J. Phys. Chem.* **1994**, *98*, 897.
(15) Yamada, T.; Batina, N.; Itaya, K. *J. Phys. Chem.* **1995**, *99*, 8817.
(16) Yamada, T.; Batina, N.; Itaya, K. *Surf. Sci.* **1995**, *335*, 204.
(17) Batina, N.; Yamada, T.; Itaya, K. *Langmuir* **1995**, *11*, 4568.
(18) Yamada, T.; Ogaki, K.; Okubo, S.; Itaya, K. *Surf. Sci.* **1996**, *369*, 321.
(19) Ocko, B. M.; Magnussen, O. M.; Wang, J. X.; Adzic, R. R.; Wandlowski, Th. *Physica B* **1996**, *221*, 238.
(20) Wan, L.-J.; Itaya, K. *Lamgmuir* **1997**, *13*, 7173.
(21) Goddard, P. J.; Lambert, R. M. *Surf. Sci.* **1977**, *67*, 180.
(22) Walter, W. K.; Manolopoulos, D. E.; Jones, R. G. *Surf. Sci.* **1996**, *348*, 115.
(23) Stickney, J. L.; Ehlers, C. B.; Gregory, B. W. *Langmuir* **1988**, *4*, 1368.
(24) Crapper, M. D.; Riley, C. E.; Sweeney, P. J. J.; McConville, C. F.; Woodruff, D. P.; Jones, R. G. *Surf. Sci.* **1987**, *182*, 213.
(25) Motai, K.; Hashizume, T.; Lu., H.; Jeon, D.; Sakurai, T. *Appl. Surf. Sci.* **1993**, *67*, 246.
(26) Suggs, D. W.; Bard, A. J. *J. Am. Chem. Soc.* **1994**, *116*, 10725.
(27) Wohlmann, B.; Park, Z.; Kruft, M.; Stuhlmann, C.; Wandelt, K.*Colloids Surf. A: Physicochem. Eng. Aspects* **1998**, *134*, 15.
(28) Lamont, C. L. A.; Conrad, H.; Bradshaw, A. M. *Surf. Sci.* **1993**, *287/288*, 169.
(29) Kadodwala, M. F.; Davis, A. A.; Scragg, G.; Cowie, B. C. C.; Kerkar, M.; Woodruff, D. P.; Jones, R. G. *Surf. Sci.* **1995**, *324*, 122.
(30) Jones, R. G.; Kadodwala, M. *Surf. Sci.* **1997**, *370*, L219.
(31) Citrin, P. H.; Eisenberger, P.; Hewitt, R. C. *Phys. Rev. Lett.* **1980**, *45*, 1948.
(32) DiCenzo, S. B.; Wertheim, G. K.; Buchanan, D. N. E. *Surf. Sci.* **1982**, *121*, 411.